

Three Flavour Majorana Neutrinos with Magnetic Moments in a Supernova

S. Esposito, V. Fiorentino, G. Mangano and G. Miele

Dipartimento di Scienze Fisiche, Università di Napoli "Federico II", and INFN, Sezione di Napoli, Mostra D'Oltremare Pad. 20, I-80125 Napoli, Italy.

Abstract

The resonant transition effects MSW and NSFP for three flavour Majorana neutrinos in a supernova are considered, where the transition magnetic moments are likely to play a relevant role in neutrino physics. In this scenario, the deformed thermal neutrino distributions are obtained for different choices of the electron-tau mixing angle. Detailed predictions for the future large neutrino detectors are also given in terms of the ratio between the spectra of recoil electrons for deformed and undeformed spectra.

PACS: 13.15.+g; 14.60.P; 13.40.Em

1 Introduction

Though the Standard Model (SM) for fundamental interactions has received a striking confirmation from experiments, the neutrino sector still remains a puzzling subject for theoretical speculations and for conceiving new experiments. The determination of the possible neutrino masses and the consequent mixing angles is the main goal of this huge scientific effort.

Several accelerator experiments have analyzed a quite wide range of the space of neutrino parameters by putting a certain number of upper bounds on these physical quantities [1]. However, it seems that the most interesting and promising observations should come from the cosmological and astrophysical side, which enables to detect extremely weak phenomena as neutrino oscillations.

In this concern, the new experimental results on solar neutrinos seem to confirm the previously observed deficit of their flux [2]. On this ground, the so-called solar neutrino problem can be reasonably considered as a well-established experimental observation. This, of course, has a number of implications on the previous question, concerning the fundamental parameters of neutrino physics (masses, mixing angles, e.m. properties). In particular, the solution of solar neutrino problem needs massive neutrinos and not vanishing mixing angles.

The mechanisms proposed to explain the deficit in the observed number of solar neutrinos with respect to the theoretical predictions of the Standard Solar Model (SSM) [3] are basically three. As far as the pure oscillation in vacuum is concerned, it is strongly disfavoured by the experimental evidence for a quite strong energy dependence of the flux depletion mechanism [4]. Certainly, the most promising solution of the solar neutrino problem is provided by the resonant oscillation mechanism, the Mikheyev-Smirnov-Wolfenstein effect (MSW) [5], which has the correct energy dependence. Nevertheless, one can imagine the superposition of a Neutrino Spin-Flavour Precession (NSFP) mechanism too [6]. This effect is relevant when a strong transverse magnetic field is present and if the magnetic dipole moments of neutrinos are large enough.

The nature of neutrinos as Dirac or Majorana particles is also still unknown. In scenarios proposed by GUT theories as $SO(10)$ [7], neutrinos are described by Majorana spinors. In this framework, since new physics is present beyond SM, the e.m. properties can also get a strong enhancement. This is in particular the case of some extended unified theories [8].

In this paper we extend the analysis recently performed by some of the present authors [9]. We will consider three-flavour Majorana neutrinos for which, due to CPT invariance, only flavour-changing magnetic dipole moments are, in general, non vanishing [8]. The resonant neutrino oscillations are considered in a supernova where the conditions of large density and strong magnetic field are likely to be obtained.

The paper is organized as follows. In section 2 we consider the effective Hamiltonian describing the interactions of three flavour Majorana neutrinos in matter. In particular we study the MSW and NSFP effects as a function of the mass difference and mixing angles. In section 3, the main supernova characteristics in terms of radial mass density profile

and magnetic field are reviewed, and the adiabaticity conditions are studied. The outcoming thermal neutrino spectra are then obtained as functions of survival and transition probabilities. In section 4 the predictions about deformed thermal neutrino spectra are obtained, and the ratio between the spectra of recoil electrons for the deformed neutrino distributions and for the unmodified ones is computed. Finally, in section 5 we give our conclusions.

2 Resonant transitions of Majorana neutrinos

For three flavour Majorana neutrinos the independent degrees of freedom, which do not take mass at the intermediate scale (10^{11} GeV) [7] and are coupled with weak interaction, can be denoted by ν_{eL} , $\nu_{\mu L}$, $\nu_{\tau L}$ and for antineutrinos by $\bar{\nu}_{eR}$, $\bar{\nu}_{\mu R}$, $\bar{\nu}_{\tau R}$. For simplicity, hereafter we will omit the indication of chirality being clear that it is left-handed for neutrinos and right-handed for antineutrinos.

In presence of a transverse magnetic dipole moment a neutrino can flip its spin and thus change its chirality. However, CPT invariance forbids these transitions for Majorana neutrinos, unless they change flavour at the same time, namely $\nu_{\alpha L} \rightarrow \bar{\nu}_{\beta R}$, with $\alpha, \beta = e, \mu, \tau$ and $\alpha \neq \beta$.

This kind of transitions are called Neutrino Spin–Flavour Precessions (NSFP) [10], and their probability can be large if the amplitudes of the transverse magnetic field and of the off-diagonal dipole magnetic moment are large enough.

As neutrino oscillations in matter (MSW), even the NSFP can receive a resonant enhancement from the presence of a dense medium [10]. This is for example the case of stellar matter or the extreme condition of a supernova.

Let us denote with ν the vector in the flavour space $\nu \equiv (\nu_e, \nu_\mu, \nu_\tau)$, and analogously $\bar{\nu} \equiv (\bar{\nu}_e, \bar{\nu}_\mu, \bar{\nu}_\tau)$. The 3×3 unitary mixing matrix can be written as [11]

$$U = \begin{pmatrix} C_\varphi C_\omega & C_\varphi S_\omega & S_\varphi \\ -C_\psi S_\omega e^{i\delta} - S_\psi S_\varphi C_\omega e^{-i\delta} & C_\psi C_\omega e^{i\delta} - S_\psi S_\varphi S_\omega e^{-i\delta} & S_\psi C_\varphi e^{-i\delta} \\ S_\psi S_\omega e^{i\delta} - C_\psi S_\varphi C_\omega e^{-i\delta} & -S_\psi C_\omega e^{i\delta} - C_\psi S_\varphi S_\omega e^{-i\delta} & C_\psi C_\varphi e^{-i\delta} \end{pmatrix}. \quad (1)$$

We will assume for simplicity $\delta = 0$, and thus U represents the mixing matrix for antineutrinos as well.

The evolution equation for neutrino wave functions travelling along the radial coordinate $r \simeq ct$ is

$$i \frac{d}{dr} \begin{pmatrix} \nu \\ \bar{\nu} \end{pmatrix} = H \begin{pmatrix} \nu \\ \bar{\nu} \end{pmatrix} = \begin{pmatrix} H_0 & B_\perp M \\ -B_\perp M & \bar{H}_0 \end{pmatrix} \begin{pmatrix} \nu \\ \bar{\nu} \end{pmatrix}. \quad (2)$$

The symmetric matrix H_0 is the 3×3 hermitian effective Hamiltonian ruling the resonant flavour transition in the flavour basis; it is given by

$$H_0 = \frac{1}{2E} U \begin{pmatrix} m_1^2 & 0 & 0 \\ 0 & m_2^2 & 0 \\ 0 & 0 & m_3^2 \end{pmatrix} U^\dagger + \begin{pmatrix} N_1(r) & 0 & 0 \\ 0 & N_2(r) & 0 \\ 0 & 0 & N_2(r) \end{pmatrix}, \quad (3)$$

where $N_1(r) = \sqrt{2}G_F(N_e - N_n/2)$, $N_2(r) = -G_F N_n/\sqrt{2}$, N_e and N_n being the electron and neutron number density, respectively. Substituting (1) in (3) we get

$$\begin{aligned}
(H_0)_{ee} &= \Sigma + N_1(r) - \Lambda S_\varphi^2 - \Delta C_{2\omega} C_\varphi^2 \quad , \\
(H_0)_{e\mu} &= -\frac{\Lambda}{2} S_{2\varphi} S_\psi + \Delta (S_{2\omega} C_\varphi C_\psi + C_{2\omega} S_\varphi S_\psi) \quad , \\
(H_0)_{e\tau} &= -\frac{\Lambda}{2} S_{2\psi} C_\varphi - \Delta \left(S_{2\omega} C_\varphi S_\psi - \frac{1}{2} C_{2\omega} S_{2\varphi} C_\psi \right) \quad , \\
(H_0)_{\mu\mu} &= \Sigma + N_2(r) - \Lambda C_\varphi^2 S_\psi^2 - \Delta \left[S_{2\omega} S_{2\psi} S_\varphi + C_{2\omega} (S_\varphi^2 S_\psi^2 - C_\psi^2) \right] \quad , \\
(H_0)_{\mu\tau} &= -\frac{\Lambda}{2} S_{2\psi} C_\varphi^2 - \Delta \left[S_{2\omega} C_{2\psi} S_\varphi + \frac{1}{2} C_{2\omega} S_{2\psi} (1 + S_\varphi^2) \right] \quad , \\
(H_0)_{\tau\tau} &= \Sigma + N_2(r) - \Lambda C_\psi^2 C_\varphi^2 + \Delta \left[S_{2\omega} S_{2\psi} S_\varphi + C_{2\omega} (S_\psi^2 - C_\psi^2 S_\varphi^2) \right] \quad , \quad (4)
\end{aligned}$$

with $\Sigma = (m_1^2 + m_2^2)/4E$, $\Delta = (m_2^2 - m_1^2)/4E$ and $\Lambda = (m_1^2 + m_2^2 - 2m_3^2)/4E$. The corresponding Hamiltonian for antineutrinos, denoted with \overline{H}_0 , is obtained from (4) by replacing $N_1(r)$, $N_2(r) \rightarrow -N_1(r)$, $-N_2(r)$. In what follows the diagonal contribution in (4) proportional to Σ can be neglected since it only gives a common phase factor.

The quantity M is the matrix of magnetic dipole moments

$$M = \begin{pmatrix} 0 & \mu_{e\mu} & \mu_{e\tau} \\ -\mu_{e\mu} & 0 & \mu_{\mu\tau} \\ -\mu_{e\tau} & -\mu_{\mu\tau} & 0 \end{pmatrix} . \quad (5)$$

The resonant conditions for transformations $\nu_e \leftrightarrow \nu_\mu$, ν_τ and for $\nu_e \leftrightarrow \overline{\nu}_\mu$, $\overline{\nu}_\tau$ can be obtained by requiring the approaching of two different eigenvalues of H in Eq.(2). For small mixing angles this essentially coincides with the condition of having coincident diagonal elements, namely, neglecting second order terms in S_ω, S_ψ and S_ϕ

$$N_1(r_s) - N_2(r_s) = 2\Delta \quad (\nu_e \leftrightarrow \nu_\mu) \quad , \quad (6)$$

$$N_1(r_s) - N_2(r_s) = \Delta - \Lambda \quad (\nu_e \leftrightarrow \nu_\tau) \quad , \quad (7)$$

$$N_1(r_s) + N_2(r_s) = 2\Delta \quad (\nu_e \leftrightarrow \overline{\nu}_\mu) \quad , \quad (8)$$

$$N_1(r_s) + N_2(r_s) = \Delta - \Lambda \quad (\nu_e \leftrightarrow \overline{\nu}_\tau) \quad . \quad (9)$$

In the same way, the resonant conditions for $\overline{\nu}_e \leftrightarrow \overline{\nu}_\mu$, $\overline{\nu}_\tau$ and for $\overline{\nu}_e \leftrightarrow \nu_\mu$, ν_τ are obtained from the charge conjugate transitions (6)-(9) by changing sign in the corresponding right hand sides. Note that r_s denotes the value of coordinate r for which each resonant condition is verified.

Once that neutrino parameters, namely mixing angles ψ , φ and ω , and Δ and Λ are fixed, one can study the occurrence of resonant conditions (6)–(9) and charged conjugate ones, by using the particular density profile for electrons and neutrons, contained in $N_1(r)$ and $N_2(r)$.

In Ref.[12] the above description for neutrino dynamics in presence of matter has been used in order to explain the solar neutrino problem. The authors assume there for

simplicity that flavour mixing occurs in the e - μ sector only. This corresponds to take in Eq.(1) $\psi, \varphi \ll \omega$ and $\delta = 0$. Thus, since ν_τ and $\bar{\nu}_\tau$ are completely decoupled, one can consider in (3) only the 2×2 matrix involving e and μ labels.

To be predictive about neutrino fluxes, one would need the precise expression for the solar magnetic field. Unfortunately, since this form is quite unknown till now, the authors consider several magnetic field configurations treated in literature.

As a result of their analysis, it is shown that for a small value of the mixing angle $\theta_{e\mu} = \omega$, $\nu_e \leftrightarrow \bar{\nu}_\mu$ transitions are sufficient to account for the solar neutrino problem. In this case the predictions strongly depend on the magnetic field configurations even if a best fit is achieved for the so-called LIN2 [12] solar magnetic field parametrization. Typical values of neutrino parameters able to reproduce the data are $\Delta m_{e\mu}^2 \simeq (10^{-8} \div 10^{-7}) eV^2$ and $\sin(2\theta_{e\mu}) \lesssim 0.2 \div 0.3$ [12].

3 Thermal neutrino spectra in a supernova

The neutrino flux dynamics contained in Eq.s(2)-(4) can be also applied to the case of a supernova. In a previous paper some of the present authors [9] already considered this situation, but in the case of negligible magnetic moments. In the following we extend that analysis in order to consider the flavour changing magnetic moment terms too.

In a supernova the mass density ranges from $\sim 10^{-5} g/cm^3$ in the external envelope up to $\sim 10^{15} g/cm^3$ in the dense core. We will assume, hereafter, the following density profile [13]

$$\rho \simeq \rho_0 \left(\frac{R_0}{r} \right)^3, \quad (10)$$

with $\rho_0 \simeq 3.5 \times 10^{10} g/cm^3$, and $R_0 \simeq 1.02 \times 10^7 cm$. The quantity R_0 denotes the radius of the so-called *neutrinosphere*, which represents the bounding surface of the region in which neutrinos of a given flavour are in thermal equilibrium. Note that, the electron fraction number Y_e outside the neutrinosphere can be assumed almost constant and fixed at the value $Y_e = 0.42$.

As far as the transverse magnetic field is concerned, one can safely assume the simple expression [14]

$$B_\perp(r) \simeq B_0 \left(\frac{R_B}{r} \right)^2, \quad (11)$$

where r denotes the radial coordinate, and the constant $B_0 R_B^2 \simeq 10^{24} \text{Gauss cm}^2$.

Here, we will assume that inside the neutrinosphere the resonance conditions are not satisfied, as suggested by predictions on neutrino mass spectrum of a wide range of unified gauge models. In first approximation neutrinos are therefore emitted from this surface with a Fermi-Dirac distribution

$$n_{\nu_\alpha}^0(E) \simeq \frac{0.5546}{T_\alpha^3} E^2 \left[1 + \exp\left(\frac{E}{T_\alpha}\right) \right]^{-1}, \quad (12)$$

with the different flavours equally populated. The index α in Eq.(12) denotes the particular neutrino species. Since the production and scattering cross-sections for electron-neutrinos are larger than for the other flavours, ν_e are produced a bit more copiously with respect to the other ones. Thus, their neutrinosphere is larger than that for ν_μ , ν_τ . This implies that the temperature T_α in (12) for the ν_e -sphere is lower than the one of ν_μ , ν_τ . Furthermore, since ν_μ and ν_τ are produced and scatter on the surrounding matter only through neutral currents, they have identical spectra. Obviously, since ν_e , ν_μ , ν_τ and $\bar{\nu}_e$, $\bar{\nu}_\mu$, $\bar{\nu}_\tau$ are produced in pairs, the magnitude of neutrino and antineutrino distributions are equal for each flavour. For the temperature of ν_e and ν_μ , ν_τ neutrinosphere we adopt the typical values $T_e \simeq 3 \text{ MeV}$ and $T_\mu = T_\tau \simeq 6 \text{ MeV}$. As far as the $\bar{\nu}_e$ distribution is concerned, it is characterized by $T_{\bar{e}} \simeq 4 \text{ MeV}$, whereas for $\bar{\nu}_\mu$ and $\bar{\nu}_\tau$ we have $T_{\bar{\mu}} = T_{\bar{\tau}} \simeq 6 \text{ MeV}$.

Assuming that the solar neutrino problem is solved in terms of $\nu_e \rightarrow \bar{\nu}_\mu$ NSFP, as explained in Ref.[12], from Eq.s(6)–(9) we see that in a supernova (for $Y_e = 0.42$ outside the neutrinosphere) four resonance conditions can be fulfilled. With decreasing density, and for τ neutrinos more massive than μ ones, we first encounter the region for e - τ resonance transitions, and then that for e - μ ones. In order we have: $\bar{\nu}_e \leftrightarrow \nu_\tau$, $\nu_e \leftrightarrow \nu_\tau$, $\bar{\nu}_e \leftrightarrow \nu_\mu$ and $\nu_e \leftrightarrow \nu_\mu$. More in detail, in the following diagram, the MSW and NSFP transitions occurring in a supernova are reported.

$$\nu_e \left\{ \begin{array}{l} \text{-----} > \nu_e \\ \text{-----} > \nu_\tau \\ \text{-----} > \nu_\mu \end{array} \right. \quad (13)$$

$$\nu_\mu \left\{ \begin{array}{l} \text{-----} > \nu_\mu \\ \text{-----} > \bar{\nu}_e \\ \text{-----} > \nu_e \end{array} \right. \quad (14)$$

$$\nu_\tau \left\{ \begin{array}{l} \text{-----} > \nu_\tau \\ \text{-----} > \bar{\nu}_e \\ \text{-----} > \nu_\mu \\ \text{-----} > \nu_e \\ \text{-----} > \nu_e \\ \text{-----} > \nu_\mu \end{array} \right. \quad (15)$$

$$\bar{\nu}_e \left\{ \begin{array}{l} \text{-----} > \bar{\nu}_e \\ \text{-----} > \nu_\mu \\ \text{-----} > \nu_e \\ \text{-----} > \nu_\tau \\ \text{-----} > \nu_e \\ \text{-----} > \nu_\mu \\ \text{-----} > \nu_e \end{array} \right. \quad (16)$$

To deduce the total transition probabilities, it is important to establish if the different resonance regions overlap, namely if the resonance widths are larger than their separation

in r . In many GUT models it is natural to expect $m_{\nu_\mu} \ll m_{\nu_\tau}$. In this paper we make this assumption, so that the resonance regions involving e - τ flavours and those involving e - μ flavours are well separated between them. For example, for 10 MeV neutrinos with $m_{\nu_\mu} \simeq 10^{-3}$ eV and $m_{\nu_\tau} \simeq 10$ eV we have the e - τ resonances around the region of density $\approx 10^8$ g/cm³ (deep in the supernova); on the contrary, the resonances e - μ is in the external envelope of supernova (≈ 1 g/cm³). Further, the MSW-NSFP resonance regions non-overlapping condition is given by [6]

$$L_\rho |\tan 2\theta_{\alpha\beta}| + \left| \frac{2\mu_{\alpha\beta} B_\perp(r_1)}{(\Delta m_{\alpha\beta}^2/2E)} \right| L_\rho \lesssim r_2 - r_1 \quad , \quad (17)$$

where r_1 is the radial position of the NSFP resonance, while r_2 is that of the MSW one, and $L_\rho \equiv -[(1/\rho)d\rho/dr]^{-1}$ is assumed to vary slowly between r_1 and r_2 . In Eq.(17) α and β label the flavours involved in the resonance ($\alpha, \beta = e, \mu, \tau$), $\theta_{\alpha\beta}$ denote the mixing angles, and $\Delta m_{\alpha\beta}^2$ is the squared mass differences of the relevant mass eigenstates. For supernova neutrinos ($E \approx 0 \div 50$ MeV), assuming (10) and (11), it is easy to see that for all models considered below, the non-overlapping condition (17) is well satisfied for both $\nu_e, \bar{\nu}_e \leftrightarrow \nu_\tau$ and $\nu_e, \bar{\nu}_e \leftrightarrow \nu_\mu$ transitions. Thus, we can conclude that the four resonances occurring in a supernova are quite well separated one each other, and as we shall see, this implies a considerable simplification, since each resonance can be considered independently from the others.

For the MSW resonance we have a simple semi-analytical formula for the survival probability [11, 16]

$$P_{\alpha\beta}(\nu_\alpha \rightarrow \nu_\alpha) = \frac{1}{2} + \left(\frac{1}{2} - \exp \left\{ -\frac{\pi}{2} \gamma_{\alpha\beta} F_{\alpha\beta} \right\} \right) \cos 2\theta_{\alpha\beta} \cos 2\theta_{\alpha\beta}^m \quad , \quad (18)$$

where the adiabaticity parameter $\gamma_{\alpha\beta}$ is given by

$$\gamma_{\alpha\beta} = \left. \frac{\Delta m_{\alpha\beta}^2 L_\rho \sin^2 2\theta_{\alpha\beta}}{2E \cos 2\theta_{\alpha\beta}} \right|_{\text{res}} \quad . \quad (19)$$

evaluated at the resonance point. In Eq.(18) $\theta_{\alpha\beta}^m$ is the effective mixing angle in matter [5, 6, 16], and is given by

$$\tan 2\theta_{\alpha\beta}^m = \frac{2\Delta m_{\alpha\beta}^2 \sin 2\theta_{\alpha\beta}}{2\sqrt{2}EG_F N_e - \Delta m_{\alpha\beta}^2 \cos 2\theta_{\alpha\beta}} \quad . \quad (20)$$

For NSFP transitions [6, 16]

$$P_{\bar{\alpha}\beta}(\bar{\nu}_\alpha \rightarrow \bar{\nu}_\alpha) = \frac{1}{2} + \left(\frac{1}{2} - \exp \left\{ -\frac{\pi}{2} \gamma_{\bar{\alpha}\beta} F_{\alpha\beta} \right\} \right) \cos 2\theta_{\alpha\beta} \cos 2\theta_{\bar{\alpha}\beta}^m \quad , \quad (21)$$

$$\gamma_{\bar{\alpha}\beta} = \left. \frac{8E\mu_{\alpha\beta}^2 B_\perp^2 L_\rho}{\Delta m_{\alpha\beta}^2} \right|_{\text{res}} \quad . \quad (22)$$

In this case the effective mixing angle in matter is

$$\tan 2\theta_{\bar{\alpha}\beta}^m = \frac{4E\mu_{\alpha\beta}B_{\perp}}{2\sqrt{2}EG_F(N_e - N_n) - \Delta m_{\alpha\beta}^2 \cos 2\theta_{\alpha\beta}} . \quad (23)$$

Note that for both the adiabatic parameters $\gamma_{\alpha\beta}$ and $\gamma_{\bar{\alpha}\beta}$ of Eq.(19) and (22), the adiabatic condition [5, 6, 16] reads

$$\gamma_{\alpha\beta}, \gamma_{\bar{\alpha}\beta} \gg 1 . \quad (24)$$

The non adiabatic correction factor $F_{\alpha\beta}$ of Eq.s(18) and (21), neglecting non adiabatic effects induced by the magnetic field with respect to those due to density [6], is given by [11]

$$F(\theta_{\alpha\beta}) \simeq \left(1 - \tan^2(\theta_{\alpha\beta})\right) \left\{ 1 + \frac{1}{3} \left[\log \left(1 - \tan^2(\theta_{\alpha\beta})\right) + 1 - \frac{1 + \tan^2(\theta_{\alpha\beta})}{\tan^2(\theta_{\alpha\beta})} \log \left(1 + \tan^2(\theta_{\alpha\beta})\right) \right] \right\} . \quad (25)$$

In terms of survival or transition probabilities, referring to diagrams (13)–(16), it is possible to write the expressions for outcoming neutrino distributions as follows

$$n_{\nu_e} = P(\nu_e \rightarrow \nu_e) n_{\nu_e}^0 + [1 - P(\nu_e \rightarrow \nu_e)] n_{\nu_x}^0 + P(\bar{\nu}_e \rightarrow \nu_e) n_{\bar{\nu}_e}^0 , \quad (26)$$

$$n_{\nu_{\mu}} + n_{\nu_{\tau}} = [1 - P(\nu_e \rightarrow \nu_e)] n_{\nu_e}^0 + [1 - P(\bar{\nu}_e \rightarrow \bar{\nu}_e) - P(\bar{\nu}_e \rightarrow \nu_e)] n_{\bar{\nu}_e}^0 + [P(\nu_e \rightarrow \nu_e) + P(\bar{\nu}_e \rightarrow \bar{\nu}_e)] n_{\nu_x}^0 , \quad (27)$$

$$n_{\bar{\nu}_e} = P(\bar{\nu}_e \rightarrow \bar{\nu}_e) n_{\bar{\nu}_e}^0 + [1 - P(\bar{\nu}_e \rightarrow \bar{\nu}_e)] n_{\nu_x}^0 , \quad (28)$$

where $n_{\nu_{\mu}}^0 = n_{\nu_{\tau}}^0 = n_{\nu_x}^0$. Note that to obtain the above expression we have only used the unitarity and the observation that $P(\nu_e \rightarrow \bar{\nu}_e)$ is vanishing (up to the first order in the mixing angle).

According to diagrams (13)–(16) the survival probabilities $P(\nu_e \rightarrow \nu_e)$ and $P(\bar{\nu}_e \rightarrow \bar{\nu}_e)$ can be written as products of the single survival probabilities at the resonances, namely

$$P(\nu_e \rightarrow \nu_e) \simeq P_{e\tau}(\nu_e \rightarrow \nu_e) P_{e\mu}(\nu_e \rightarrow \nu_e) , \quad (29)$$

$$P(\bar{\nu}_e \rightarrow \bar{\nu}_e) \simeq P_{\bar{e}\tau}(\bar{\nu}_e \rightarrow \bar{\nu}_e) P_{\bar{e}\mu}(\bar{\nu}_e \rightarrow \bar{\nu}_e) . \quad (30)$$

while the transition probability $P(\bar{\nu}_e \rightarrow \nu_e)$ takes the expression

$$P(\bar{\nu}_e \rightarrow \nu_e) \simeq P_{\bar{e}\tau}(\bar{\nu}_e \rightarrow \bar{\nu}_e) [1 - P_{\bar{e}\mu}(\bar{\nu}_e \rightarrow \bar{\nu}_e)] [1 - P_{e\mu}(\nu_e \rightarrow \nu_e)] + P_{e\mu}(\nu_e \rightarrow \nu_e) [1 - P_{\bar{e}\tau}(\bar{\nu}_e \rightarrow \bar{\nu}_e)] [1 - P_{e\tau}(\nu_e \rightarrow \nu_e)] . \quad (31)$$

Note that all the expressions (29)–(31) are obtained under the assumption that the single resonances of diagrams (13)–(16) are well separated.

4 Numerical results

According to the above results (26)–(28), the deformed thermal neutrino spectra are obtained once that neutrino parameters are fixed.

For the electron–muon sector, the relevant parameters can be fixed according to the explanation assumed for the solar neutrino problem. In this paper, since we are interested in a possible scenario in which the neutrino electromagnetic properties play the essential role we will choose the NSFP explanation [12]. In this case, the deficit in the solar neutrino flux is mainly due to the conversion $\nu_e \rightarrow \bar{\nu}_\mu$, being assumed Majorana neutrinos, which is the natural choice occurring in GUT theories where a see-saw mechanism is at work. The alternative scenario of a pure MSW explanation was treated by some of the present authors in a previous paper [9].

In the NSFP framework, the values for neutrino parameters able to reproduce the data are $\Delta m_{e\mu}^2 \simeq 10^{-8} \text{ eV}^2$ and $\sin(2\theta_{e\mu}) \simeq 0.2$ and $\mu_{e\mu} \simeq 10^{-11} \mu_B$ [12].

Concerning the parameters for the electron–tau sector, they are less constrained. However, we can fix $\Delta m_{e\tau}^2 \simeq m_{\nu_\tau}^2 \simeq 25 \text{ eV}^2$ in order to be able to identify ν_τ has the hot component of dark matter [17], whereas, for the transition magnetic moment we can assume $\mu_{e\tau}$ to be of the same order of $\mu_{e\mu}$, since, typically, the enhancement to the electromagnetic properties is due to physics beyond the electroweak interactions, which hardly distinguishes between τ –leptons and μ –leptons. Hence, the only remaining parameters is $\theta_{e\tau}$, for which we will choose three indicative values, namely, 10^{-1} , 10^{-4} and 10^{-8} . Values in this range are for example predicted by SUSY GUT theories [18], where one could expect in principle an enhancement of the neutrino electromagnetic properties.

In Figures 1–3, we show the deformed neutrino distributions for ν_e , the sum of ν_μ and ν_τ , and $\bar{\nu}_e$ distributions, respectively, versus their initial distributions. In all figures, the solid line represents the initial distribution and the predictions for the outgoing neutrino distributions are obtained for the above three values of $\theta_{e\tau}$. Furthermore, in Figure 4, we plot the adiabaticity parameters $\gamma_{e\mu}$, $\gamma_{e\tau}$ and $\gamma_{\bar{e}\mu}$, $\gamma_{\bar{e}\tau}$ of eqs. (19) and (22). In particular the dashed line represents $\gamma_{e\tau}$ for the two cases $\theta_{e\tau} = 10^{-1}$ (upper line) and $\theta_{e\tau} = 10^{-4}$ (lower line).

As one can see from Figure 4, for $\theta_{e\tau} = 10^{-1}$ the MSW $\nu_e \leftrightarrow \nu_\tau$ transition is the only one to be adiabatic, and thus the $\nu_e \rightarrow \nu_\tau$ conversion is the only one which provides an efficient reshuffling of initial distributions. It corresponds (dashed line in Figure 1) to a depletion of ν_e distribution in favour of ν_τ (dashed line of Figure 2). Note, however, that the adiabaticity of MSW transitions (19) decreases with neutrino energy, whereas it increase for NSFP (22).

The MSW $\nu_e \leftrightarrow \nu_\tau$ conversion becomes less and less efficient as $\theta_{e\tau}$ decreases, as can be seen by the other two lines in Figures 1 and 2. For the other values of $\theta_{e\tau}$, in fact, $\gamma_{e\tau} \ll 1$. However, as one can see from the dashed-dotted line of Figure 1, corresponding to the extremely small value $\theta_{e\tau} = 10^{-8}$, a conversion of ν_e in other kind of neutrinos still remains. In fact, in this case the only conversions remaining are the NSFP as one can see by observing the antineutrinos spectra of Figure 3. Note that since we have fixed $\mu_{e\mu} \sim \mu_{e\tau} \sim 10^{-11} \mu_B$, all the deformed antineutrino distributions are almost coincident,

because, in this case, they are almost independent of the on neutrino mixing angles (see Eq.s.(21)–(23)).

The distortions in the neutrino and/or antineutrino energy spectra can be observed in the future large neutrino detectors, now under constructions, like SuperKamiokande and SNO. To quantify our predictions on directly observable quantities, let us consider for example the ν - e^- elastic scattering for neutrino detection. A relevant quantity, which measures the deformation on neutrino distributions due to resonant transitions is the ratio between the recoil electron spectrum for deformed neutrino distributions and the undeformed one. It is defined as

$$R(T, E_\nu^{th}) = \frac{S(T, E_\nu^{th})}{S^0(T, E_\nu^{th})} \quad , \quad (32)$$

where

$$\begin{aligned} S(T, E_\nu^{th}) = & k \left\{ \int_{E_\nu^{th}}^{E_{max}} \left[n_{\nu_e}(E) \frac{d\sigma}{dT}(\nu_e e^- \rightarrow \nu_e e^-) + n_{\bar{\nu}_e}(E) \frac{d\sigma}{dT}(\bar{\nu}_e e^- \rightarrow \bar{\nu}_e e^-) \right. \right. \\ & + \left(n_{\nu_\mu}(E) + n_{\nu_\tau}(E) \right) \frac{d\sigma}{dT}(\nu_\mu (\nu_\tau) e^- \rightarrow \nu_\mu (\nu_\tau) e^-) \\ & \left. \left. + \left(n_{\bar{\nu}_\mu}(E) + n_{\bar{\nu}_\tau}(E) \right) \frac{d\sigma}{dT}(\bar{\nu}_\mu (\bar{\nu}_\tau) e^- \rightarrow \bar{\nu}_\mu (\bar{\nu}_\tau) e^-) \right] dE \right\} \quad , \quad (33) \end{aligned}$$

E_ν^{th} being the neutrino energy threshold, while E_{max} is the endpoint in the neutrino spectra, and $S^0(T, E_\nu^{th})$ is defined as (33), but for the initial distributions. Note that R is independent of the factor k which contains the information about the percentage of supernova neutrino reaching the detector and other reduction factors due to the detector set up. For the explicit expressions of the differential cross sections occurring in (33) see for example Ref.[19].

In Figure 5, R is shown for the three values of θ_{er} considered, by assuming for simplicity a vanishing neutrino energy threshold and $E_{max} = 50 \text{ MeV}$.

5 Conclusions

In this paper we have studied the deformation of thermal neutrino spectra emitted from a supernova due to resonant transition effects. In particular we have considered three flavour light Majorana neutrinos, as suggested by GUT theories like SO(10) for the neutrino degrees of freedom not taking mass at the intermediate scale ($\sim 10^{11} \text{ GeV}$), according to the see-saw mechanism [7].

In the present analysis, which represents an extension of a previous study in which MSW transitions were considered only, we have assumed enhanced electromagnetic neutrino properties, as suggested by several unified models and by the NSFP solution to the SNP. Thus, the supernova outcoming neutrinos experience spin flavour precessions [10] in addition to the usual MSW phenomena [5].

We have calculated the deformed neutrino spectra once neutrino parameters, like masses, mixing angles and transitional magnetic moments are fixed (CPT invariance forbids diagonal magnetic moments for Majorana neutrinos). In this scenario, since we are interested in a situation in which the enhanced electromagnetic moments play an essential role in neutrino physics, we assume the results obtained in Ref.[12], where the deficit in the solar neutrino flux is explained in terms of the NSFP conversion $\nu_e \rightarrow \bar{\nu}_\mu$. Thus, from the experimental data one can obtain all the parameters of e - μ sector. As far as the e - τ sector is concerned, the magnetic transitional moment $\mu_{e\tau}$ can be reasonably fixed to be of the order of $\mu_{e\mu}$, since the enhancement should be due to physics beyond the electroweak interaction and thus it is reasonable to assume that it should contribute in a comparable way to all leptonic families. Furthermore, requiring that ν_τ is the hot component of DM [17], its mass can be fixed equal to 5 eV.

For three choices of ν_e - ν_τ mixing angle, we have then explicitly obtained the deformed ν_e , $\nu_\mu + \nu_\tau$ and $\bar{\nu}_e$ energy spectra, as reported in Figures 1–3. Finally, our predictions for a directly observable quantity, such as the ratio R defined in Eq.(32) have been given in Figure 5.

Acknowledgements

We thank Prof. F. Buccella for valuable comments and remarks.

References

- [1] R.M. Barnett et al., *Phys. Rev D* **54** (1996) 1.
- [2] R. Davis Jr., Proc. of the 23rd ICRC, Calgary, Canada (1993), *Prog. in Nucl. and Part. Phys.* **32** (1994);
K. Hirata et al, *Phys. Rev.* **D44** (1991) 2241;
A. Abazov et al, *Phys. Rev. Lett.* **67** (1991) 3332;
P. Anselmann et al., *Phys. Lett.* **B327** (1994) 377.
- [3] J.N. Bahcall, *Neutrino Astrophysics*, (Cambridge University Press, 1989).
- [4] See, for example, S. Esposito, *Mod. Phys. Lett.* **A8** (1993) 1557.
- [5] L. Wolfenstein, *Phys. Rev.* **D17** (1978) 236;
S.P. Mikheyev and A.Yu. Smirnov, *Nuovo Cim.* **C9** (1986) 17; *Sov. J. Nucl. Phys.* **42** (1986) 913; *Sov. Phys. Usp.* **30** (1987) 759.
- [6] E.Kh. Akhmedov, *Sov. Phys. JETP* **68** (1989) 690.
- [7] F. Buccella and L. Rosa, *Z. Phys.* **C36** (1987) 425;
M.F. Abud, F. Buccella, L. Rosa and A. Sciarrino, *Z. Phys.* **C44** (1989) 589;
R.N. Mohapatra and M.K. Parida, *Phys. Rev.* **D47** (1993) 264;
F. Acampora, G. Amelino-Camelia, F. Buccella, O. Pisanti, L. Rosa, and T. Tuzi, *Nuovo Cim.* **A108** (1995) 375;

- G. Amelino-Camelia, O. Pisanti and L. Rosa, *Nucl. Phys. (Proc. Suppl.)* **B43** (1995) 86;
 K.S. Babu and R.N. Mohapatra, *Phys. Rev. Lett.* **70** (1993) 2845;
 Dae-Gyu Lee and R.N. Mohapatra, *Phys. Lett.* **B329** (1994) 463.
- [8] See for example R. Mohapatra and P.B. Pal, *Massive Neutrinos in Physics and Astrophysics*, (World Scientific, Singapore, 1991).
- [9] F. Buccella, S. Esposito, C. Gualdi and G. Miele, *Z. Phys.* **C73** (1997) 633.
- [10] M.B. Voloshin, M.I. Vysotskii and O.B. Okun', *Zh. Eksp. Teor. Fiz.* **91** (1986) 754 [*Sov. Phys. JETP* **64** (1986) 446];
 E. Kh. Akhmedov, preprint IAE-4568/I, January 1988;
 E. Kh. Akhmedov, *Phys. Lett.* **B213** (1988) 64;
 C.S. Lim and W.J. Marciano, *Phys. Rev.* **D37** (1988) 1368;
 E. Kh. Akhmedov and O.V. Bychuk, *Zh. Eksp. Teor. Fiz.* **95** (1989) 442 [*Sov. Phys. JETP* **68** (1989) 250].
- [11] T.K. Kuo and J. Pantaleone, *Rev. Mod. Phys.* **61** (1989) 937.
- [12] E.Kh. Akhmedov, A. Lanza and S.T. Petcov, *Phys. Lett.* **B348** (1995) 124.
- [13] T. Janka and W. Hillebrandt, *Astron. Astroph. Suppl.* **78** (1989) 375.
- [14] S. Sahu, V.B. Semikoz and J.W.F. Valle, preprint hep-th/9512390.
- [15] W.C. Haxton, *Phys. Rev.* **D36** (1987) 2283.
- [16] K. Ahmed and M.A. Mughal, *Mod. Phys. Lett.* **A9** (1994) 2097.
- [17] G.B. Gelmini, hep-ph/9606409;
 Q. Shafi and F. Stecker, *Phys. Rev. Lett.* **53** (1984) 1292;
 C.P. Ma and E. Bertscihinger, *Ap. J.* **429** (1994) 22, and *Ap. J.* **434** (1994) L5;
 J. Primak et al., *Phys. Rev. Lett.* **74** (1995) 2160.
- [18] S. Dimopoulos, L. S. Hall and S. Raby, *Phys. Rev.* **D47** (1993) 3697;
 Y. Achiman and T. Greiner, *Nucl. Phys.* **B443** (1995) 3;
 Dae-Gyu Lee and R.N. Mohapatra, *Phys. Rev.* **D51** (1995) 1353.
- [19] L.B. Okun, *Leptons and Quarks*, (North Holland, Amsterdam, 1987).

Fig. 1

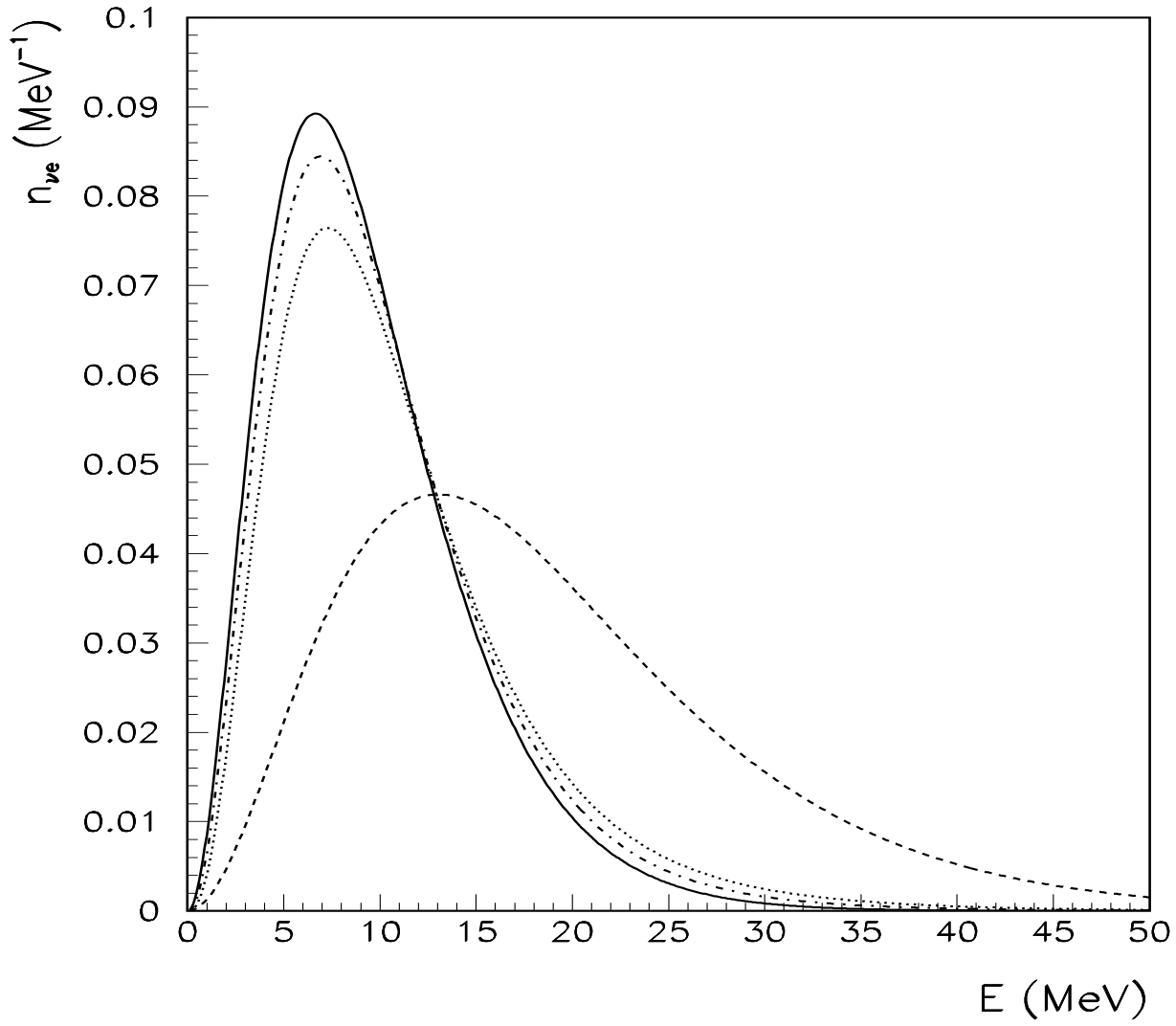


Figure 1: The energy spectra for ν_e versus energy are reported. The solid line represents the initial distribution, whereas the dashed line corresponds to the distorted spectra for $\theta_{e\tau} = 10^{-1}$. The dotted line and dashed-dotted correspond to $\theta_{e\tau} = 10^{-4}$ and 10^{-8} , respectively.

Fig. 2

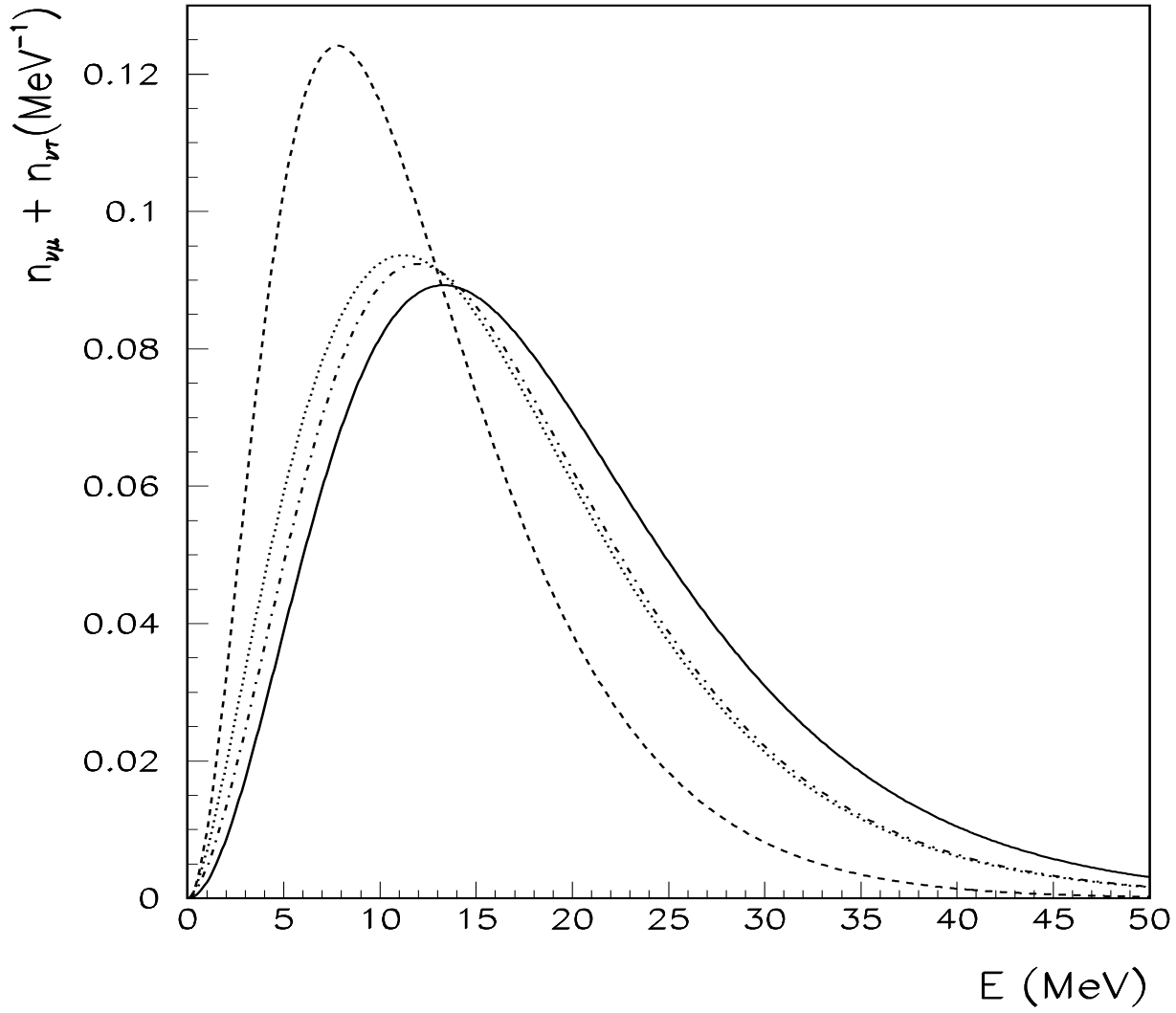


Figure 2: The energy spectra for $n_{\nu\mu} + n_{\nu\tau}$, with the same notation of Figure 1,

Fig. 3

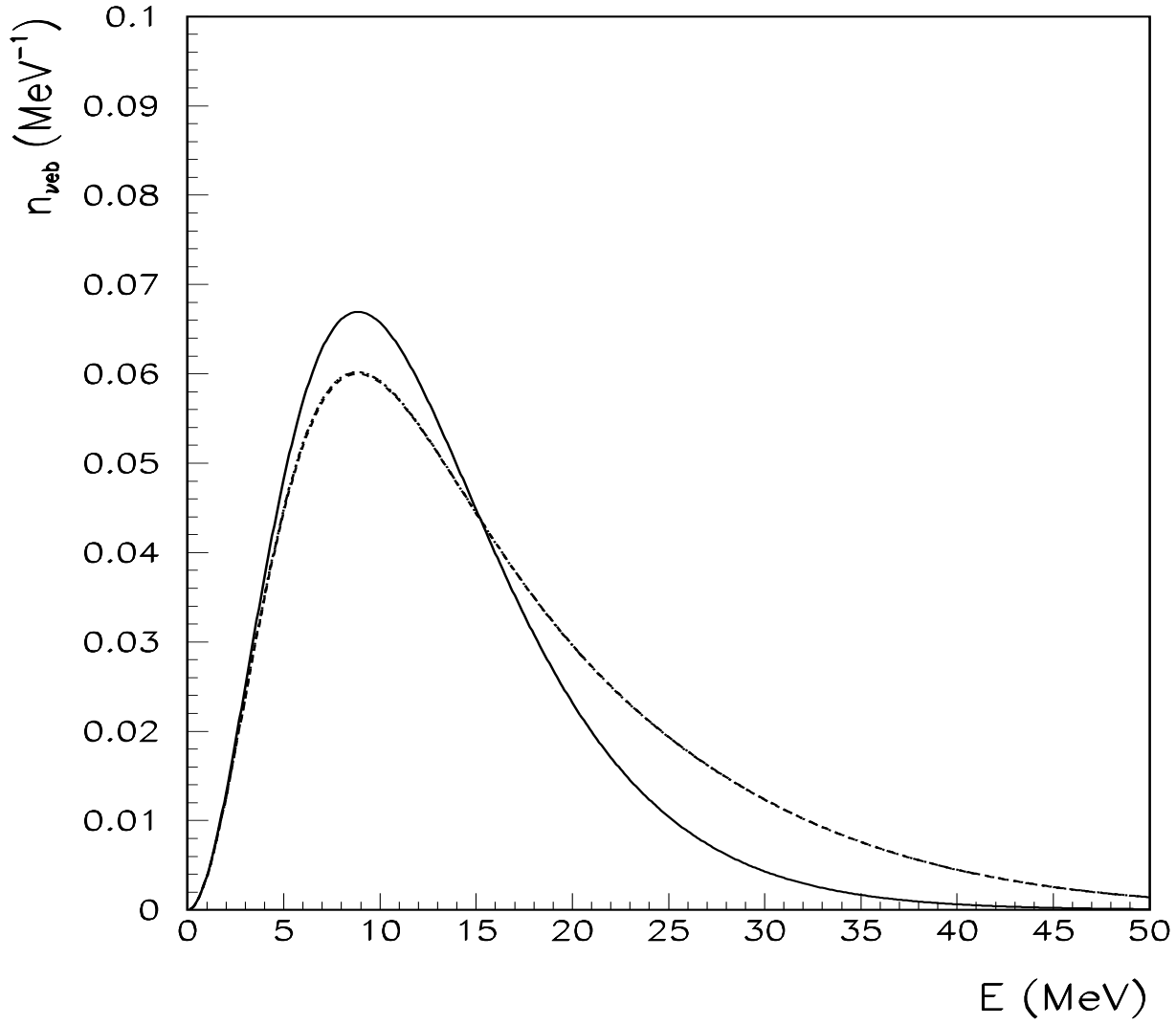


Figure 3: The energy spectra for $n_{\bar{\nu}_e}$, with the same notation of Figure 1

Fig. 4

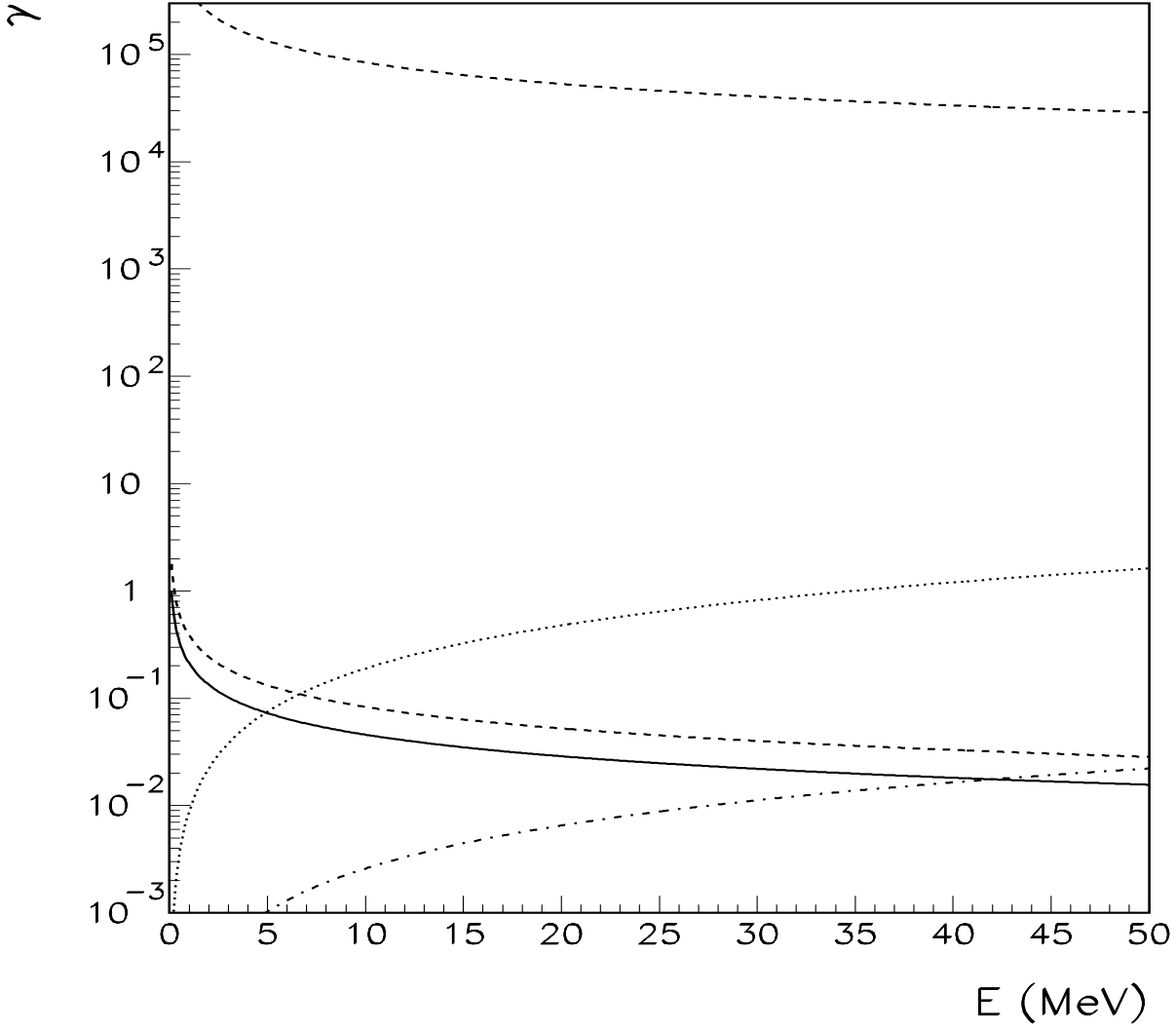


Figure 4: Energy dependence of the adiabaticity parameters $\gamma_{\alpha\beta}$ and $\gamma_{\bar{\alpha}\beta}$ of eqs. (19) and (22). The solid line represents $\gamma_{e\mu}$ and the dashed lines $\gamma_{e\tau}$: the upper one corresponds to $\theta_{e\tau} = 10^{-1}$ and the lower to $\theta_{e\tau} = 10^{-4}$. The dotted line is $\gamma_{\bar{e}\mu}$ and the dashed-dotted represents $\gamma_{\bar{e}\tau}$.

Fig. 5

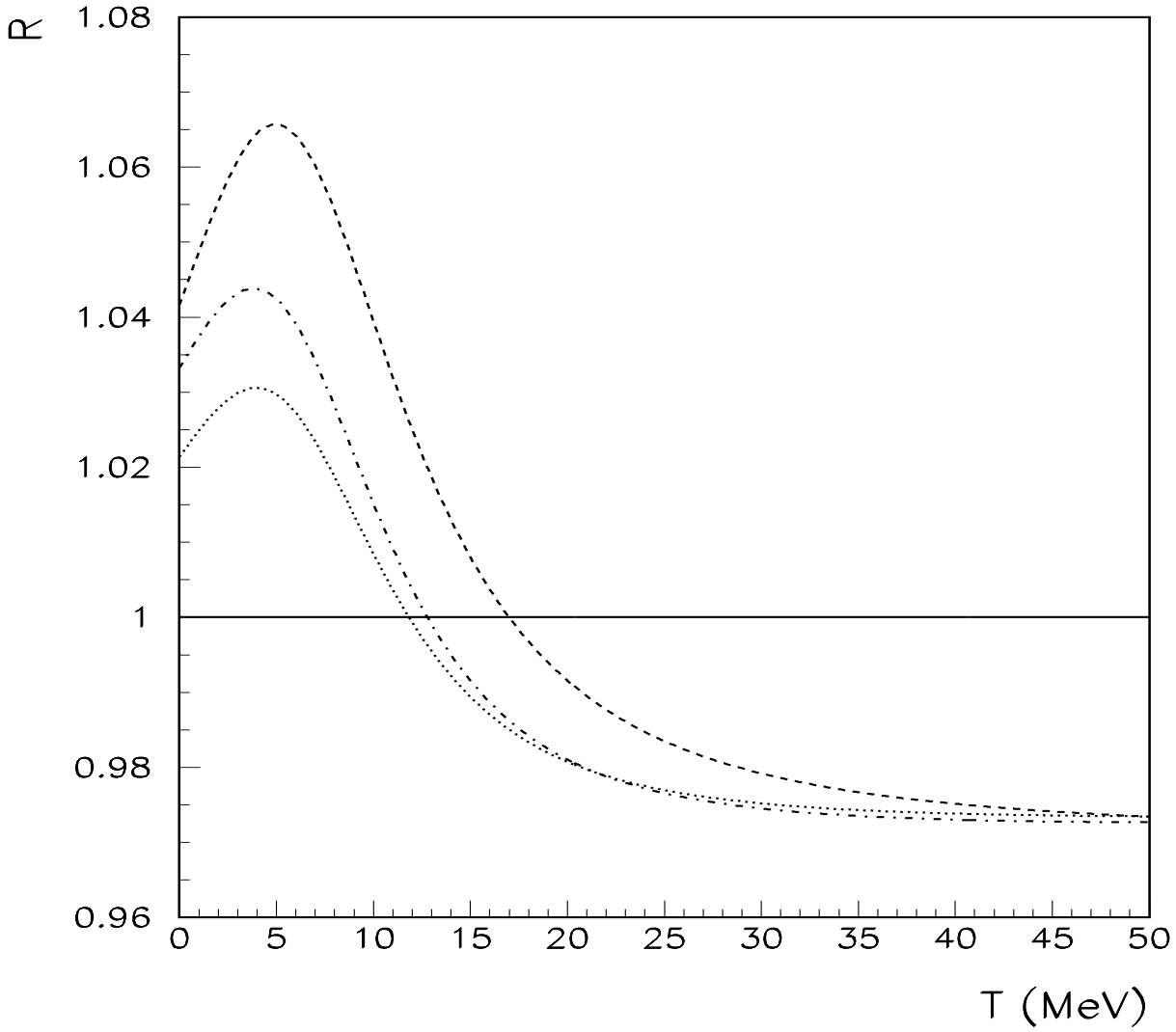


Figure 5: The ratio R (see Eq.(32)) is plotted for $\theta_{e\tau} = 10^{-1}$ (dashed line), 10^{-4} (dotted line) and 10^{-8} (dashed-dotted line). For simplicity a vanishing neutrino energy threshold has been used.